OPEN ACCESS



Spin Doctors: How to Diagnose a Hierarchical Merger Origin

Ethan Payne ^{1,2}, Kyle Kremer ^{3,6}, and Michael Zevin ^{4,5},

Department of Physics, California Institute of Technology, Pasadena, CA 91125, USA; epayne@caltech.edu

LIGO Laboratory, California Institute of Technology, Pasadena, CA 91125, USA

TAPIR, California Institute of Technology, Pasadena, CA 91125, USA

Adler Planetarium, 1300 South DuSable Lake Shore Drive, Chicago, IL 60605, USA

Center for Interdisciplinary Exploration and Research in Astrophysics (CIERA), Northwestern University, Evanston, IL 60201, USA

Received 2024 February 22; revised 2024 April 11; accepted 2024 April 13; published 2024 April 26

Abstract

Gravitational-wave observations provide the unique opportunity of studying black hole formation channels and histories—but only if we can identify their origin. One such formation mechanism is the dynamical synthesis of black hole binaries in dense stellar systems. Given the expected isotropic distribution of component spins of binary black holes in gas-free dynamical environments, the presence of antialigned or in-plane spins with respect to the orbital angular momentum is considered a tell-tale sign of a merger's dynamical origin. Even in the scenario where birth spins of black holes are low, hierarchical mergers attain large component spins due to the orbital angular momentum of the prior merger. However, measuring such spin configurations is difficult. Here, we quantify the efficacy of the spin parameters encoding aligned-spin ($\chi_{\rm eff}$) and in-plane spin (χ_p) at classifying such hierarchical systems. Using Monte Carlo cluster simulations to generate a realistic distribution of hierarchical merger parameters from globular clusters, we can infer mergers' $\chi_{\rm eff}$ and χ_p . The cluster populations are simulated using Advanced LIGO-Virgo sensitivity during the detector network's third observing period and projections for design sensitivity. Using a "likelihood-ratio"-based statistic, we find that $\sim 2\%$ of the recovered population by the current gravitational-wave detector network has a statistically significant χ_p measurement, whereas no $\chi_{\rm eff}$ measurement was capable of confidently determining a system to be antialigned with the orbital angular momentum at current detector sensitivities. These results indicate that measuring spin-precession through χ_p is a more detectable signature of hierarchical mergers and dynamical formation than antialigned spins.

Unified Astronomy Thesaurus concepts: Stellar mass black holes (1611); Gravitational waves (678); Star clusters (1567); Bayesian statistics (1900)

1. Introduction

Following the first handful of observations of binary black hole (BBH) mergers through their gravitational-wave (GW) emission (Abbott et al. 2016, 2019, 2021), many studies predicted that the dominant formation channel of BBHs would be determined after $\mathcal{O}(10\text{--}100)$ observations (Stevenson et al. 2015; Fishbach & Holz 2017; Gerosa & Berti 2017; Stevenson et al. 2017; Vitale et al. 2017; Zevin et al. 2017; Arca Sedda & Benacquista 2019; Safarzadeh 2020; Gerosa & Fishbach 2021). However, despite the LIGO-Virgo-KAGRA Collaboration (LVK) detector network accumulating nearly 100 confident BBH observations (Abbott et al. 2023a), prominent formation pathways for BBH mergers remain an open question in GW astrophysics. The incongruity between prior expectation and reality can be attributed to a number of factors:

- 1. The diversity in the GW events detected thus far does not show a strong preference for any one formation channel, with observations spanning a broad range of masses and mass ratios (e.g., Abbott et al. 2019, 2021; Olsen et al. 2022; Abbott et al. 2023a; Mehta et al. 2023).
- 2. Additional potential formation channels have been proposed in addition to the canonical "dynamical-

Original content from this work may be used under the terms of the Creative Commons Attribution 4.0 licence. Any further distribution of this work must maintain attribution to the author(s) and the title of the work, journal citation and DOI.

- versus-isolated" distinction (see, e.g., Mandel & Farmer 2022 for a review), as well as subchannels to these canonical birth environments, which muddles the ability to pin down specific birth environments (Cheng et al. 2023).
- 3. Uncertainties in massive-star evolution, binary physics, and formation environments are more vast than previously appreciated, translating to larger uncertainties in expected parameter distributions and generally making inference difficult (see, e.g., Mapelli 2021; Spera et al. 2022 for reviews).
- 4. Unlike black holes (BHs) in high-mass X-ray binaries in the Milky Way, which have been argued to have spin estimates that are near extremal (Liu et al. 2008; Miller-Jones et al. 2021; Reynolds 2021), the population of spins for GW-detected BHs are relatively small (Abbott et al. 2021), making it difficult to distinguish between small, aligned spins expected from isolated evolution and moderate, in-plane spins expected from dynamical assembly.

In addition to spins, trends in the mass spectrum (e.g., Stevenson et al. 2015; Zevin et al. 2017; Fishbach et al. 2021; Belczynski et al. 2022; Mahapatra et al. 2022; Abbott et al. 2023b; van Son et al. 2023), redshift evolution (e.g., Rodriguez & Loeb 2018; van Son et al. 2022; Fishbach & van Son 2023), orbital eccentricity (e.g., Zevin et al. 2021b), and correlations between BBH parameters (e.g., Callister et al. 2021; Adamcewicz & Thrane 2022; Biscoveanu et al. 2022; Broekgaarden et al. 2022; McKernan et al. 2022; Tiwari 2022;

⁶ NASA Hubble Fellow.

Zevin & Bavera 2022; Baibhav et al. 2023; Ray et al. 2023) have been investigated to elucidate the contribution of the various proposed BBH formation channels, although a robust conclusion is still far from being reached.

Although the holistic approach of examining features of the full BBH population holds promise for constraining formation scenarios (Zevin et al. 2021a), a complementary approach is the identification of individual merger events with distinguishing features uniquely associated with one or a subset of formation pathways. One example of this is eccentricity: BBH mergers with measurable eccentricity in the LVK sensitive frequency range (≥ 0.05 at 10 Hz; Lower et al. 2018; Romero-Shaw et al. 2019) strongly point to a recent dynamical interaction, as orbital eccentricity quickly dissipates if a BBH system inspirals over a long timescale. Although no eccentric BBH mergers have been confidently detected to date (though see Romero-Shaw et al. 2022), the detection of a small number of eccentric mergers (or nondetection of eccentric mergers) would place stringent constraints on the contribution of dynamical formation pathways (Zevin et al. 2021b).

Another possible smoking-gun signal of dynamical formation is the presence of hierarchical mergers—BBH mergers where one or both of the component BHs have gone through a previous merger event. Hierarchical mergers have masses that are typically larger than their "first-generation" progenitors that were born from massive stars as well as distinctive signatures in their spin magnitudes ($a \approx 0.7$, with a dispersion based on the mass ratio and component spins of the prior merger) and spin orientations (an isotropic distribution assuming a gas-free dynamical formation environment). Although hierarchical mergers are predicted to contain BHs with masses in the (pulsational) pair instability mass gap and studies have attempted to quantify the likelihood of particular GW systems being hierarchical mergers (Kimball et al. 2020a, 2020b, 2021; Mahapatra et al. 2021), uncertainties in the size and location of the gap (Farmer et al. 2019; Edelman et al. 2021; Abbott et al. 2023b), measurement uncertainties for high-mass BHs (Abbott et al. 2020), and prior considerations (Fishbach & Holz 2020; Nitz & Capano 2021; Mould et al. 2023) make mass alone difficult to pin down whether a particular system contains a BH that was the result of a prior merger.

To identify the tell-tale signatures of hierarchical mergers, it is useful to consider the leading-order (i.e., typically best-measured) spin terms from the post-Newtonian expansion of the GW waveform: the effective spin (Damour 2001; Racine 2008)

$$\chi_{\text{eff}} = \frac{a_1 \cos \theta_1 + q a_2 \cos \theta_2}{1 + q},\tag{1}$$

and precessing spin (Schmidt et al. 2015)

$$\chi_p = \max \left(a_1 \sin \theta_1, \, q \frac{3 + 4q}{4 + 3q} a_2 \sin \theta_2 \right)$$
(2)

parameters, where q is the mass ratio between the secondary and primary BHs, and a_1 and a_2 are the primary and secondary BHs' spins, respectively. The effective spin encodes a mass-weighted projection of the spin vectors on the orbital angular momentum axis, whereas χ_p depends on the projection of the spin vector on the plane of the orbit and is related to the strength of precession of the orbital angular momentum about the total angular momentum.

Hierarchical mergers are expected to have distinctive signatures in both of these spin parameters, due to generally large spin magnitudes (acquired during their first-generation merger; Buonanno et al. 2008; Fishbach et al. 2017) and isotropic spin orientations (a natural feature of dynamical formation in gas-poor environments, e.g., Rodriguez et al. 2019), some hierarchical mergers should show evidence for negative $\chi_{\rm eff}$, and others for large χ_p . While a positive $\chi_{\rm eff}$ is possible, such systems may not be distinguishable from other formation channels whereas spin antialignment is difficult to form in the field (Rodriguez et al. 2016). Being a typically better-measured parameter (Ng et al. 2018; Biscoveanu et al. 2021), studies have focused on negative $\chi_{\rm eff}$ as a potential sign for a hierarchical merger event (e.g., Baibhav et al. 2020; Fishbach et al. 2022; Zhang et al. 2023). However, due to the inherent isotropic spin orientation distribution that is expected for hierarchical mergers in most astrophysical environments, many more systems will have large in-plane spins as opposed to large spins antialigned with the orbital angular momentum. For example, from cluster population simulations (see Section 2), $\sim 0.5\%$ ($\sim 20\%$) of hierarchical systems will have $\chi_{\rm eff} < -0.5$ ($\chi_{\rm eff} < -0.2$), whereas $\sim 67\%$ ($\sim 96\%$) of systems will have $\chi_p > 0.5$ ($\chi_p > 0.2$). So while $\chi_{\rm eff}$ is expected to be better measured, a significantly higher fraction of the hierarchical population will have the distinct signature of

In this Letter, we investigate the ability to measure each of these parameters for the purpose of identifying specific BBH mergers that are likely of a hierarchical origin. We take synthetic BBH mergers from realistic models of globular clusters, performing full parameter estimation on 6×10^3 events. Using these realistic measurement uncertainties, we quantify the fraction of hierarchical mergers that confidently exhibit negative $\chi_{\rm eff}$ and large χ_p . Despite larger typical measurement uncertainties, we show that χ_p is a better indicator of hierarchical mergers than $\chi_{\rm eff}$ —a consequence of the generic properties of hierarchically formed BBHs.

The remainder of this Letter is as follows. We outline the cluster population models used to construct the simulated set of first-generation (1G1G) and hierarchical BBH mergers in Section 2 before discussing how we quantify the measurements of the spin parameters in Section 3.1. The results of this calculation using the simulated population of BBH mergers as well as a selection of observed GW signals are presented in Section 3.2. Finally, concluding remarks and implications of this study are presented in Section 4.

2. Cluster Population Models

We assemble our synthetic sample of dynamically formed BBH mergers using the CMC Cluster Catalog, a suite of *N*-body cluster simulations spanning the parameter space of globular clusters observed in the local Universe (Kremer et al. 2020). This catalog of models is computed using CMC (Rodriguez et al. 2022), a Hénon-type Monte Carlo code that includes various physical processes specifically relevant to the dynamical formation of BH binaries in dense star clusters including two-body relaxation, stellar and binary evolution (computed using COSMIC; Breivik et al. 2020), and direct integration of small-*N* resonant encounters including post-Newtonian effects (Rodriguez et al. 2018). In total, this catalog contains 148 independent simulations with variation in total cluster mass, initial virial radius, metallicity, and cluster

truncation due to galactic tidal forces. The chosen values for these parameters reflect the observed properties of the Milky Way globular clusters (e.g., Harris 1996), but also serve as reasonable proxies for extragalactic clusters (e.g., Brodie & Strader 2006) enabling a robust exploration of the formation of GW sources in dense star clusters throughout the local Universe.

To obtain a realistic astrophysically weighted sample of BBH mergers, we follow Rodriguez & Loeb (2018) and Zevin et al. (2021b): each of the 148 simulations are placed into equally spaced bins in cluster mass and logarithmically spaced bins in metallicity. Each cluster model is then assigned a relative astrophysical weight corresponding to the number of clusters expected to form in its associated 2D mass-metallicity bin across cosmic time, assuming that the initial cluster masses follow a $\propto M^{-2}$ distribution (e.g., Lada & Lada 2003) and that metallicities (as well as corresponding cluster formation times) follow the hierarchical assembly distributions of El-Badry et al. (2019). For all BBH mergers in a given model, the drawn cluster formation time is then added to the BH binary's merger time, yielding a realistic distribution of BBH merger events as a function of redshift. This scheme yields a predicted BBH merger rate of roughly 20 Gpc⁻³ yr⁻¹ in the local Universe from dense star clusters.

We account for detectability of the simulated binary systems by generating colored Gaussian noise corresponding to a three-detector LIGO-Virgo GW detector network at both design sensitivity (Aasi et al. 2015; Acernese et al. 2015) and at the sensitivity the network achieved during the first half of LVK's third observing period (O3; Abbott et al. 2021). We then add the simulated signals, randomly generating the binary's orientation and sky position, to the detector network noise and calculate the matched-filter signal-to-noise ratio (S/N; Cutler & Flanagan 1994). Signals which pass the threshold S/N of 10 are kept within the set of simulated detections.

In the CMC simulations, all BHs formed via stellar evolution are assumed to have negligible birth spin, a reasonable assumption if angular momentum transport in their massivestar progenitors is highly efficient (e.g., Qin et al. 2018; Fuller & Ma 2019). However, spin can be imparted to cluster BHs through previous BH merger events (Buonanno et al. 2008). We assume all spin tilts are isotropically distributed. In addition to the nonspinning first-generation mergers, we consider two additional populations—the population of hierarchical BBHs formed consistently from these nonspinning first-generation systems, and first-generation mergers with BH spins artificially included between [0, 0.2]. The latter population is included as a "worst-case" scenario for first-generation mergers that are not formed with small spins. While we do not self-consistently generate a fourth population corresponding to hierarchical mergers from this spinning first-generation population, modifications to the spin properties of first-generation BHs only marginally change the distribution of hierarchical merger parameters (see Figures 4, 6, and 7 from Rodriguez et al. 2019). The dominant impact of a spinning first-generation population is a significant reduction in the rate of hierarchical mergers, which does not affect our conclusions significantly regarding distinguishing the mergers within the hierarchical population but would affect their rates via the number of systems that are retained (Rodriguez et al. 2019; Mahapatra et al. 2021; Zevin & Holz 2022).

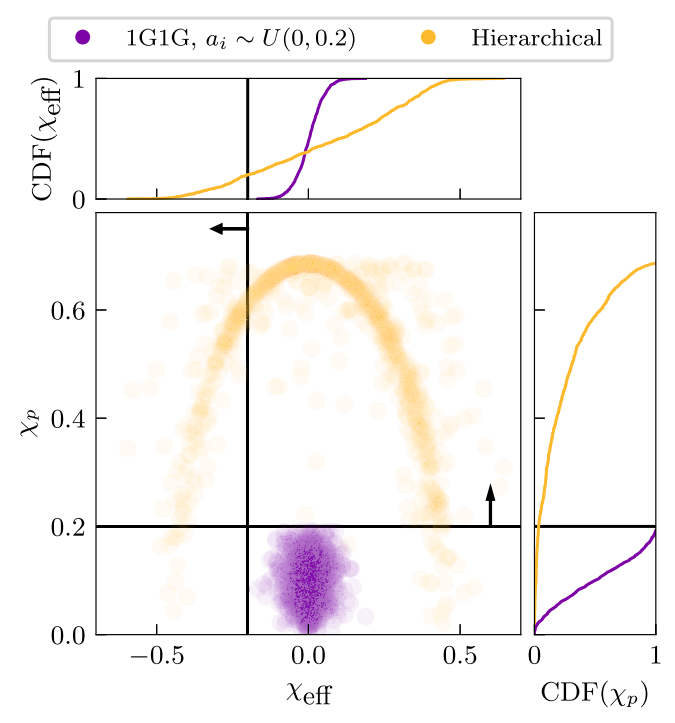


Figure 1. Two-dimensional distribution of spin parameters, $\chi_{\rm eff}$ and χ_p , for detectable low-spinning first-generation BBHs (1G1G; purple), and hierarchically formed BBHs (yellow). The one-dimensional marginal cumulative distribution functions (CDFs) are shown in the top and right panels. The spins of the low-spinning population are drawn uniformly and isotropically with spin-magnitudes from 0 to 0.2 in postprocessing. All black hole masses are determined from the cluster simulations. We have selected for signals that are detectable by enforcing a signal-to-noise ratio threshold of 10 across the three detector LIGO-Virgo network at the LVK's sensitivity during their third observing period. The threshold of $\chi_{\rm thres}=0.2$ used throughout the manuscript is indicated by the black lines for $\chi_{\rm eff}$ and χ_p . A significantly greater fraction of the hierarchical systems possess $\chi_p > 0.2$ than $\chi_{\rm eff} < -0.2$.

In Figure 1 we show the spin parameters, $\chi_{\rm eff}$ and χ_p , of the O3-detected set of simulations from the low-spinning first-generation (purple), and hierarchical BBHs. The black lines indicate reasonable thresholds beyond which no 1G1G systems reside in the $\chi_{\rm eff}$ - χ_p parameter space. While χ_p is typically less well-measured in GW observations (Ng et al. 2018; Biscoveanu et al. 2021), hierarchical systems overwhelmingly produce more moderate-to-high χ_p BBHs and occupy a unique region of the $\chi_{\rm eff}$ - χ_p plane (Baibhav et al. 2021). Therefore, in the following section, we explore the use of both $\chi_{\rm eff}$ and χ_p as potential "smoking-gun" signatures of a BBH's hierarchical origin.

3. Distinguishing Hierarchical Mergers

In this section, we turn our attention to how we might observationally identify the hierarchical mergers predicted from cluster populations using only the effective and precession spin parameters inferred from the observed GW signals. We first outline how we quantify the significance of the measurement before applying the calculation to the simulated cluster populations following Section 2 in addition to a number of GW events from the LVK's third observing period, which may present evidence of hierarchical origin based on their leading-order spin measurements.

3.1. Quantifying Spin Measurement Significance

To understand the detectability of χ_p and $\chi_{\rm eff}$ in the simulated populations produced in Section 2, we infer the 15 binary parameters (assuming quasi-circular orbits) for each merger injected into the two GW networks considered. We then calculate the posterior distributions on $\chi_{\rm eff}$ and χ_p directly from the inferred spin parameters, using Equations (1) and (2).

To quantify how significantly $\chi_{\rm eff}$ and χ_p are measured beyond the chosen thresholds, we utilize a "likelihood-ratio"-based statistic, denoted LR. This threshold boundary is somewhat arbitrary but can be motivated from the cluster simulations in Section 2. We compute LR by integrating over the marginal single-event likelihood and a uniform prior bounded between the threshold and the parameter boundaries (here denoted χ_L and χ_U for the lower and upper edges, respectively). For example,

$$LR_{\chi \leqslant \chi_{\text{thres}}}^{\chi > \chi_{\text{thres}}} = \frac{\int_{\chi_{\text{thres}}}^{\chi_U} \mathcal{L}(d|\chi) U(\chi_{\text{thres}}, \chi_U) d\chi}{\int_{\chi_L}^{\chi_{\text{thres}}} \mathcal{L}(d|\chi) U(\chi_L, \chi_{\text{thres}}) d\chi}$$
(3)

computes the likelihood ratio for support above the threshold, χ_{thres} , compared to below the threshold. Here, $\mathcal{L}(d|\chi)$ is the marginal likelihood for the observed event data, d, given the spin parameter χ (either χ_p or $\chi_{\rm eff}$). We use the analytical expressions from Callister (2021) to construct the marginal likelihood (i.e., all prior dependence, $\pi(\chi|q)$, is removed). It is important to note, however, that in marginalizing over all other degrees of freedom we have made implicit choices for the prior distributions on other parameters, such as the individual BH masses and redshift. We use uniform-in-detector-frame component mass priors when sampling in chirp mass and mass ratio (Romero-Shaw et al. 2020; Callister 2021), and a Euclidean luminosity distance prior ($\propto d_I^2$). While these choices will inevitably have an impact on the inferred LR values, we are aiming to identify unequivocally spinning systems. Equation (3) can also be inverted to compute the likelihood ratio for support below the threshold.

Upon close examination of Equation (3), astute readers would note that it closely resembles a Bayes factor between two possible hypotheses (a spin parameter either above or below $\chi_{\rm thres}$). Therefore, we can interpret the inferred value in a similar way—the likelihood ratio quantifies the amount of support above (below) the threshold against the support below (above) it. A common metric in the field of Bayesian statistics is that a ${\rm lnLR}_{\chi \leq \chi_{\rm thres}}^{\chi > \chi_{\rm thres}} > 8$ quantifies significant evidence, corresponding to a ~ 3000 :1 preference for $\chi > \chi_{\rm thres}$ (Jeffreys 1961). Due to the nature of this calculation, there is statistical uncertainty due to a finite number of posterior distribution samples above $\chi_{\rm thres}$. The uncertainty in ${\rm ln LR}$ scales approximately, ignoring the impact of the removal of the prior, as $\sim \sqrt{{\rm LR}/N}$, where N in the posterior samples. Since we have $\sim 40,000$ samples per event, this corresponds to an

$$LR_{\chi \leqslant \chi \text{thres}}^{\chi > \chi \text{thres}} = \frac{\int_{\chi \text{thres}}^{\chi_U} p(\chi|d) d\chi}{\int_{\chi \text{thres}}^{\chi \text{thres}} p(\chi|d) d\chi}$$
(4)

could be computed instead, where $p(\chi|d)$ is the marginal posterior distribution.

uncertainty of ~ 0.3 at $\ln LR = 8$. This may slightly modify the exact percentage of systems passing the chosen $\ln LR = 8$ threshold, though the broader conclusions of the Letter are unaffected.

There are, of course, many other parameters and methods to quantify this significance (Fairhurst et al. 2020a, 2020b; Gerosa et al. 2021; Thomas et al. 2021). Here we utilize this straightforward approach for two reasons. The first is that it is intuitive to interpret from the one-dimensional marginal distribution how much support is above or below a threshold? And the second is that this statistic is more directly understood by the leading order terms in the GW radiation due to both $\chi_{\rm eff}$ and χ_p , rather than being related first to the noise properties as in Fairhurst et al. (2020a, 2020b). Therefore, with a choice of spin threshold for the LR ($\chi_{\rm thres}$; motivated by Section 2) and under the assumption that all systems that pass $\chi_{\rm thres}$ are hierarchical mergers, we can use measurements of LR as a proxy for a definitive detection of a hierarchical merger. A $\chi_{\rm thres}$ value of 0.2 is motivated by confidently bounding observations above the expected small spins from Qin et al. (2018) and Fuller & Ma (2019). We further choose more conservative thresholds $(\chi_{\text{thres}} = 0.3, 0.4)$ in the case where first-generation BHs might have some mechanism of being spun up (e.g., Ma & Fuller 2023). However, these systems still typically possess spins below 0.4 and are rare (e.g., see Appendix A.1.3 of Zevin et al. 2021a). Additionally, it is expected that the presence of hierarchical mergers formed from first-generation BBH mergers with birth spins above 0.2 is heavily suppressed due to the ejection of the merger remnant from the cluster environment (Rodriguez et al. 2019). Finally, the more conservative bound of $\chi_{\rm thres} = 0.4$ is consistent with the population observed thus far by the LVK (Abbott et al. 2023b) being consistent with only first-generation BHs. This measure relies heavily on only the spins of the system, and so the statements in the following sections are conservative. Information about the masses could be incorporated to boost the significance, though a threshold on masses will then need to be chosen as well, may be less motivated given large uncertainties in the underlying firstgeneration mass distributions (e.g., Mapelli 2021; Spera et al. 2022), and will inadvertently remove lighter hierarchical systems from consideration.

3.2. Application to Cluster Population Models

To explore how effectively hierarchical mergers can be selected out from a given population using spin parameters, we infer the properties of 1000 mergers from each of the three simulated populations (1G1G, 1G1G with uniform spin magnitudes in the range [0, 0.2], and hierarchical systems; as described in Section 2) in the current GW detector network (from the third observing period; Abbott et al. 2021) and at design sensitivity (Aasi et al. 2015; Acernese et al. 2015). We simulate these signals using the gravitational waveform model IMRPHENOMXPHM (Pratten et al. 2021), which we add into Gaussian noise colored by the respective noise power spectral densities. We arrive at 6000 posterior distributions, using the nested sampling algorithm dynesty (Speagle 2020) embedded within the Bayesian inference library Bilby (Ashton et al. 2019; Romero-Shaw et al. 2020), from which we calculate the LR following Equation (3). From these results, we can then construct the complementary cumulative

⁷ We have opted for the terminology "likelihood ratio" here as we are removing the explicit and complex behavior of the posterior distribution with respect to the prior. If interested,

Publicly available posterior samples are available at 10.5281/zenodo.10558308.

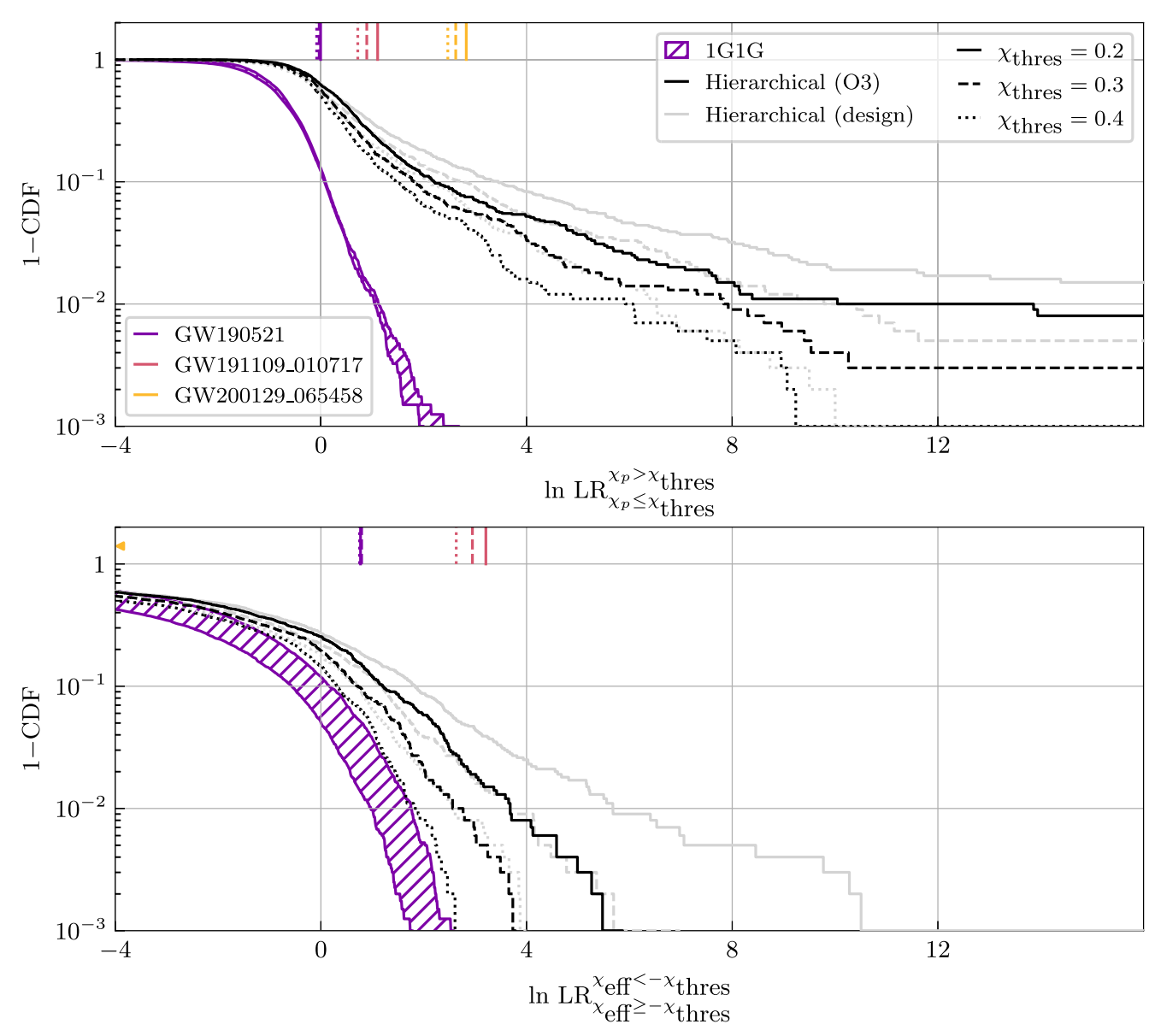


Figure 2. The complementary cumulative distribution function (1–CDF) of detectable 1G1G (shaded; purple) and hierarchical BBH mergers (lines) as a function of the logarithmic likelihood ratio, $\ln LR$, defined in Equation (3). The three different line styles correspond to different threshold choices ($\chi_{thres} = 0.2, 0.3, 0.4$), and shadings correspond to simulated signals detected in the first half of the LVK's third observing period (O3) sensitivity (dark), or a three-detector LIGO-Virgo network at design sensitivity (light). The top and bottom panels correspond to the complementary cumulative distribution functions for χ_p and χ_{eff} , respectively. Finally, the observed values of $\ln LR$ at the different thresholds for three gravitational-wave observations made during O3—GW190521 (purple), GW191109_010717 (pink), and GW200129_065458 (yellow)—are marked. A significantly larger fraction of the hierarchical population possesses a confidently measurable value of χ_p , whereas only the most relaxed threshold at design sensitivity can lead to a confident negative χ_{eff} measurement in a single event.

distribution function indicating the recovered fraction of observations that have an LR above a given value. The result of this calculation is shown in Figure 2 for both χ_p (top) and $\chi_{\rm eff}$ (bottom). We find little difference in the inferred distribution of values of LR for 1G1G systems, independent of detector sensitivity and only slightly dependent on the choice of threshold and spin distribution. We therefore group all such possible distributions into the hatched purple region in Figure 2. The fractions of hierarchical binaries for different thresholds are shown in black and gray for LVK's GW detector network at O3 sensitivity and at design sensitivity, respectively. The complementary cumulative distribution function as a function of the LR represents the fraction of simulated observations above an LR value. Finally, we also include the relevant values from three GW observations with ticks above

the curves: GW190521 (purple; Abbott et al. 2020a, 2020, 2024), GW191109_010717 (pink), and GW200129_065458 (yellow; Abbott et al. 2023a).

From Figure 2, we can identify the fraction of hierarchical binaries that pass a particular threshold of likelihood ratio for both χ_p and $\chi_{\rm eff}$. Focusing on observations in the third LVK observing period (O3), ~2% of hierarchical mergers possess $\ln LR_{\chi_p > 0.2}^{\chi_p > 0.2} > 8$, indicating a confident detection. S/N plays a mild impact on the systems with high LRs, with higher S/N systems somewhat more likely to have higher LRs. For example, 15% of hierarchical systems have S/N >20, whereas 63% of all hierarchical systems with $\ln LR_{\chi_p > 0.2}^{\chi_p > 0.2} > 4$ possess an S/N > 20. We anticipate much of the support for higher values of χ_p in these systems is also a product of clear imprints

of spin precession in the waveform from specific spin configurations. However, no choice of χ_{thres} can provide a confident measurement for negative $\chi_{\rm eff}$ except with the most liberal threshold ($\chi_{\rm thres}=0.2$) at the design sensitivity of the three-detector LIGO-Virgo detector network. Therefore, from the simulated population of BBH mergers from globular clusters, $\chi_{\rm eff}$ is a wholly ineffectual parameter for distinguishing individual⁹ hierarchical mergers.¹⁰ Furthermore, if we instead treat the 1G1G population as a "null" background distribution from which to define a threshold (which is a very liberal threshold—requiring complete confidence in the population model), we still arrive at similar conclusions. With a detection threshold informed from the 1G1G LR distribution (ln LR $_{\chi \leq 0.2}^{\chi > 0.2} >$ 3), we find $\sim 8\%$ of hierarchical mergers would be distinguishable via precession effects, while only $\sim 3\%$ would be distinguishable from $\chi_{\rm eff}$ measurements. While we believe it to be difficult to claim any one observation is of a hierarchical origin with $ln LR \sim 3$, an ensemble of such observations would indicate some number of these observations were hierarchical. This may lead to hints at the level of a population of hierarchical BBH mergers in the LVK's current fourth observing period—even if we are not confident in the origin of any one event.

Finally, we briefly turn our attention to a select few events from the LVK's third observing period (O3) that have been discussed in the literature as potential systems with anti- or misaligned spins—GW190521, GW191109_010717, and GW200129_065458 (Abbott et al. 2020, 2020b, 2021, 2023a, 2024). For simplicity and direct comparison to the simulated mergers, we use only posteriors constructed using IMRPHE-NOMXPHM. Using the LR calculation, no events surpass ln LR > 8 for either χ_p or $\chi_{\rm eff}$, although with a reduced threshold of ln LR > 3, GW200129_065458 and GW191109_010717 pass the thresholds for χ_p and $\chi_{\rm eff}$, respectively. However, since the impact of data quality issues impacting the interpretation of these events is still an open question, caution should be taken when interpreting these results (see Davis et al. 2022; Payne et al. 2022; Macas et al. 2024; Udall & Davis 2023).

4. Conclusions

Unequivocal detections of a hierarchical BBH merger via GW observations will help understand the formation channels and histories of such systems. While studies often focus on identifying a hierarchical merger from antialigned spins (see, e.g., Fishbach et al. 2022; Zhang et al. 2023), we have focused on both the measurement of spin-precession in addition to antialignment in a simulated BBH merger population from realistic cluster models (Rodriguez et al. 2022). From this study, the key insights are as follows:

 We have demonstrated that, in a realistic cluster population, determining a system to be hierarchical will

- likely first come from the measurement of spin-precession (see Figure 2).
- 2. Additionally, from these simulated BBH mergers from 1G1G and hierarchical systems, we can approximately discern the number of GW observations needed to uncover a hierarchical system in such a manner. We generally find that we should not yet have expected to confidently identify a hierarchical merger. Since ~25% of the detectable BBHs from the cluster population are hierarchical, and ~2% are confidently detectable at the current sensitivity of the GW network (from Figure 2), there is only a 25% chance one or more hierarchical mergers would have been detectable in the LVK's third observing run (Abbott et al. 2021, 2023a, 2024). This probability should be considered a generous upper limit, as it assumes dynamical formation in globular clusters as the only channel and environment.
- 3. Future observations appear much more fruitful. At design sensitivity, $\sim\!4\%$ of hierarchical mergers become distinguishable. With an increased number of detections (ranging from $\sim\!200$ to 1000; Kiendrebeogo et al. 2023), one can reasonably expect $\sim\!2$ –10 identifiably hierarchical systems. Crucially, this analysis cannot be undertaken using antialignment of spins (i.e., $\chi_{\rm eff}$), as such effects will not be detectable, even in the most optimistic of circumstances.

As the ground-based GW detector network evolves and approaches its design sensitivity, the tangible possibility of observing an unequivocally spinning, hierarchical merger will become a reality. As we enter this era, the conclusions drawn here will be important in future discussions about the hierarchical origins of yet-to-be-detected BBH mergers. When discussing such a system, in this Letter we find it will be significantly more advantageous to investigate the spin-precession than spin misalignment. This motivates current and future research into both population modeling for hierarchical systems (and their first-generation progenitors) and waveform modeling to accurately capture this effect.

Acknowledgments

The authors thank Zoheyr Doctor, Christopher Berry, and Parthapratim Mahapatra for their insightful comments on the Letter. Support for K.K. was provided by NASA through the NASA Hubble Fellowship grant HST-HF2-51510 awarded by the Space Telescope Science Institute, which is operated by the Association of Universities for Research in Astronomy, Inc., for NASA, under contract NAS5-26555. M.Z. gratefully acknowledges funding from the Brinson Foundation in support of astrophysics research at the Adler Planetarium.

The authors are grateful for computational resources provided by the LIGO Laboratory and supported by National Science Foundation Grants PHY-0757058 and PHY-0823459. This material is based upon work supported by NSF's LIGO Laboratory, which is a major facility fully funded by the National Science Foundation. LIGO was constructed by the California Institute of Technology and Massachusetts Institute of Technology with funding from the National Science Foundation and operates under cooperative agreement PHY-1764464. This paper carries LIGO Document Number LIGO-P2400050.

This does not invalidate hierarchical studies where a population of potentially antialigned systems may be identified, as more information is extracted from a population of sources (e.g., Abbott et al. 2021; Fishbach et al. 2022; Miller et al. 2024).

¹⁰ We also computed LR with the primary BH spin magnitude (a_1) . We find that ~4% of hierarchical mergers possess $\ln LR_{q_1\leq 0.2}^{a_1>0.2}>8$. While insightful, this does not factor in spin alignment and therefore such a measure may be contaminated by other channels.

While GW190521 (Abbott et al. 2021) and GW200129_065458 (Hannam et al. 2022; Abbott et al. 2023a) have results with waveform models more closely resembling numerical relativity (NRSUR7DQ4; Varma et al. 2019), using these samples for these two results only marginally affects these conclusions.

Software: Bilby (Ashton et al. 2019; Romero-Shaw et al. 2020); dynesty (Speagle 2020); iPython (Pérez & Granger 2007); Matplotlib (Hunter 2007); NumPy (Harris et al. 2020); Pandas (Wes McKinney 2010); SciPy (Virtanen et al. 2020).

ORCID iDs

Ethan Payne https://orcid.org/0000-0003-4507-8373 Kyle Kremer https://orcid.org/0000-0002-4086-3180 Michael Zevin https://orcid.org/0000-0002-0147-0835

References

```
Aasi, J., et al. 2015, CQGra, 32, 074001
Abbott, B. P., et al. 2016, PhRvL, 116, 241102
Abbott, B. P., et al. 2019, PhRvX, 9, 031040
Abbott, R., Abbott, T. D., Abraham, S., et al. 2020a, PhRvL, 125, 101102
Abbott, R., Abbott, T. D., Abraham, S., et al. 2021, ApJL, 913, L7
Abbott, R., et al. 2020b, ApJL, 900, L13
Abbott, R., et al. 2021, PhRvX, 11, 021053
Abbott, R., et al. 2023a, PhRvX, 13, 041039
Abbott, R., et al. 2023b, PhRvX, 13, 011048
Abbott, R., et al. 2024, PhRvD, 109, 022001
Acernese, F., et al. 2015, CQGra, 32, 024001
Adamcewicz, C., & Thrane, E. 2022, MNRAS, 517, 3928
Arca Sedda, M., & Benacquista, M. 2019, MNRAS, 482, 2991
Ashton, G., et al. 2019, ApJS, 241, 27
Baibhav, V., Berti, E., Gerosa, D., Mould, M., & Wong, K. W. K. 2021,
   PhRvD, 104, 084002
Baibhav, V., Doctor, Z., & Kalogera, V. 2023, ApJ, 946, 50
Baibhav, V., Gerosa, D., Berti, E., et al. 2020, PhRvD, 102, 043002
Belczynski, K., Doctor, Z., Zevin, M., et al. 2022, ApJ, 935, 126
Biscoveanu, S., Callister, T. A., Haster, C.-J., et al. 2022, ApJL, 932, L19
Biscoveanu, S., Isi, M., Varma, V., & Vitale, S. 2021, PhRvD, 104, 103018
Breivik, K., Coughlin, S., Zevin, M., et al. 2020, ApJ, 898, 71
Brodie, J. P., & Strader, J. 2006, ARA&A, 44, 193
Broekgaarden, F. S., Stevenson, S., & Thrane, E. 2022, ApJ, 938, 45
Buonanno, A., Kidder, L. E., & Lehner, L. 2008, PhRvD, 77, 026004
Callister, T. 2021, arXiv:2104.09508
Callister, T. A., Haster, C.-J., Ng, K. K. Y., Vitale, S., & Farr, W. M. 2021,
   ApJL, 922, L5
Cheng, A. Q., Zevin, M., & Vitale, S. 2023, ApJ, 955, 127
Cutler, C., & Flanagan, E. E. 1994, PhRvD, 49, 2658
Damour, T. 2001, PhRvD, 64, 124013
Davis, D., Littenberg, T. B., Romero-Shaw, I. M., et al. 2022, CQGra, 39,
  245013
Edelman, B., Doctor, Z., & Farr, B. 2021, ApJL, 913, L23
El-Badry, K., Quataert, E., Weisz, D. R., Choksi, N., & Boylan-Kolchin, M.
   2019, MNRAS, 482, 4528
Fairhurst, S., Green, R., Hannam, M., & Hoy, C. 2020a, PhRvD, 102, 041302
Fairhurst, S., Green, R., Hoy, C., Hannam, M., & Muir, A. 2020b, PhRvD,
   102, 024055
Farmer, R., Renzo, M., de Mink, S. E., Marchant, P., & Justham, S. 2019, ApJ,
   887, 53
Fishbach, M., Doctor, Z., Callister, T., et al. 2021, ApJ, 912, 98
Fishbach, M., & Holz, D. E. 2017, ApJL, 851, L25
Fishbach, M., & Holz, D. E. 2020, ApJL, 904, L26
Fishbach, M., Holz, D. E., & Farr, B. 2017, ApJL, 840, L24
Fishbach, M., Kimball, C., & Kalogera, V. 2022, ApJL, 935, L26
Fishbach, M., & van Son, L. 2023, ApJL, 957, L31
Fuller, J., & Ma, L. 2019, ApJL, 881, L1
Gerosa, D., & Berti, E. 2017, PhRvD, 95, 124046
Gerosa, D., & Fishbach, M. 2021, NatAs, 5, 749
Gerosa, D., Mould, M., Gangardt, D., et al. 2021, PhRvD, 103, 064067
Hannam, M., et al. 2022, Natur, 610, 652
Harris, C. R., Millman, K. J., van der Walt, S. J., et al. 2020, Natur, 585, 357
Harris, W. E. 1996, AJ, 112, 1487
Hunter, J. D. 2007, CSE, 9, 90
Jeffreys, H. 1961, Theory of Probability (3rd edn.; Oxford: Oxford Univ. Press)
```

```
Kimball, C., Talbot, C., Berry, C. P. L., et al. 2020b, ApJ, 900, 177
Kimball, C., Talbot, C., Berry, C. P. L., et al. 2021, ApJL, 915, L35
Kremer, K., Ye, C. S., Rui, N. Z., et al. 2020, ApJS, 247, 48
Lada, C. J., & Lada, E. A. 2003, ARA&A, 41, 57
Liu, J., McClintock, J. E., Narayan, R., Davis, S. W., & Orosz, J. A. 2008,
    pJL, 679, L37
Lower, M. E., Thrane, E., Lasky, P. D., & Smith, R. 2018, PhRvD, 98, 083028
Ma, L., & Fuller, J. 2023, ApJ, 952, 53
Macas, R., Lundgren, A., & Ashton, G. 2024, PhRvD, 109, 062006
Mahapatra, P., Gupta, A., Favata, M., Arun, K. G., & Sathyaprakash, B. S.
   2021, ApJL, 918, L31
Mahapatra, P., Gupta, A., Favata, M., Arun, K. G., & Sathyaprakash, B. S.
  2022, arXiv:2209.05766
Mandel, I., & Farmer, A. 2022, PhR, 955, 1
Mapelli, M. 2021, Handbook of Gravitational Wave Astronomy, ed. C. Bambi,
  S. Katsanevas, & K. D. Kokkotas (Singapore: Springer), 16
McKernan, B., Ford, K. E. S., Callister, T., et al. 2022, MNRA
Mehta, A. K., Olsen, S., Wadekar, D., et al. 2023, arXiv:2311.06061
Miller, S. J., Ko, Z., Callister, T. A., & Chatziioannou, K. 2024, arXiv:2401.
Miller-Jones, J. C. A., Bahramian, A., Orosz, J. A., et al. 2021, Sci, 371, 1046
Mould, M., Gerosa, D., Dall'Amico, M., & Mapelli, M. 2023, MNRAS,
  525, 3986
Ng, K. K. Y., Vitale, S., Zimmerman, A., et al. 2018, PhRvD, 98, 083007
Nitz, A. H., & Capano, C. D. 2021, ApJL, 907, L9
Olsen, S., Venumadhav, T., Mushkin, J., et al. 2022, PhRvD, 106, 043009
Payne, E., Hourihane, S., Golomb, J., et al. 2022, PhRvD, 106, 104017
Pérez, F., & Granger, B. E. 2007, CSE, 9, 21
Pratten, G., et al. 2021, PhRvD, 103, 104056
Qin, Y., Fragos, T., Meynet, G., et al. 2018, A&A, 616, A28 Racine, É. 2008, PhRvD, 78, 044021
Ray, A., Magaña Hernandez, I., Mohite, S., Creighton, J., & Kapadia, S. 2023,
  ApJ, 957, 37
Reynolds, C. S. 2021, ARA&A, 59, 117
Rodriguez, C. L., Amaro-Seoane, P., Chatterjee, S., et al. 2018, PhRvD, 98,
  123005
Rodriguez, C. L., & Loeb, A. 2018, ApJL, 866, L5
Rodriguez, C. L., Weatherford, N. C., Coughlin, S. C., et al. 2022, ApJS,
Rodriguez, C. L., Zevin, M., Amaro-Seoane, P., et al. 2019, PhRvD, 100,
  043027
Rodriguez, C. L., Zevin, M., Pankow, C., Kalogera, V., & Rasio, F. A. 2016,
   ApJL, 832, L2
Romero-Shaw, I., Lasky, P. D., & Thrane, E. 2022, ApJ, 940, 171
Romero-Shaw, I. M., Lasky, P. D., & Thrane, E. 2019, MNRAS, 490, 5210
Romero-Shaw, I. M., et al. 2020, MNRAS, 499, 3295
Safarzadeh, M. 2020, ApJL, 892, L8
Schmidt, P., Ohme, F., & Hannam, M. 2015, PhRvD, 91, 024043
Speagle, J. S. 2020, MNRAS, 493, 3132
Spera, M., Trani, A. A., & Mencagli, M. 2022, Galax, 10, 76
Stevenson, S., Berry, C. P. L., & Mandel, I. 2017, MNRAS, 471, 2801
Stevenson, S., Ohme, F., & Fairhurst, S. 2015, ApJ, 810, 58
Thomas, L. M., Schmidt, P., & Pratten, G. 2021, PhRvD, 103, 083022
Tiwari, V. 2022, ApJ, 928, 155
Udall, R., & Davis, D. 2023, ApPhL, 122, 094103
van Son, L. A. C., de Mink, S. E., Callister, T., et al. 2022, ApJ, 931, 17
van Son, L. A. C., de Mink, S. E., Chruślińska, M., et al. 2023, ApJ, 948, 105
Varma, V., Field, S. E., Scheel, M. A., et al. 2019, PhRvR, 1, 033015
Virtanen, P., Gommers, R., Oliphant, T. E., et al. 2020, NatMe, 17, 261
Vitale, S., Lynch, R., Sturani, R., & Graff, P. 2017, CQGra, 34, 03LT01
Wes McKinney 2010, in Proc. of the 9th Python in Science Conf., ed.
  S. van der Walt & J. Millman, 56
Zevin, M., & Bavera, S. S. 2022, ApJ, 933, 86
Zevin, M., Bavera, S. S., Berry, C. P. L., et al. 2021a, ApJ, 910, 152
Zevin, M., & Holz, D. E. 2022, ApJL, 935, L20
Zevin, M., Pankow, C., Rodriguez, C. L., et al. 2017, ApJ, 846, 82
Zevin, M., Romero-Shaw, I. M., Kremer, K., Thrane, E., & Lasky, P. D.
  2021b, ApJL, 921, L43
Zhang, R. C., Fragione, G., Kimball, C., & Kalogera, V. 2023, ApJ, 954, 23
```

Kiendrebeogo, R. W., et al. 2023, ApJ, 958, 158

Kimball, C., Berry, C. P. L., & Kalogera, V. 2020a, RNAAS, 4, 2